Effect of Grain Size on Dynamic Recrystallization and Hot-Ductility Behaviors in High-Nitrogen CrMn Austenitic Stainless Steel

ZHENHUA WANG, SHUHUA SUN, BO WANG, ZHONGPING SHI, RONGHUA ZHANG, and WANTANG FU

The dynamic recrystallization and hot-ductility behaviors in fine- and coarse-grained 18Mn18Cr0.5N steel were determined between 1273 K and 1473 K (1000 °C and 1200 °C) at a strain rate of 0.1 s^{-1} through compression and tensile tests. The microstructure was examined using optical microscopy, electron backscatter diffraction analysis, and transmission electron microscopy. The fracture morphology was observed using scanning electron microscopy. The coarse initial grain size delays the initiation and development of dynamic recrystallization and then results in a lower hot ductility. The nucleation of dynamic recrystallization grains at triple junctions and at grain boundaries is mainly accompanied by the evolution of twinning and low-angle grain boundaries, respectively. The nucleation mechanism of dynamic recrystallization grains affects the dynamic recrystallization grain size. Dynamic recrystallization grains evolved by the necklace mechanism are coarser than those evolved by the ordinary mechanism. The hot ductility of 18Mn18Cr0.5N steel is very sensitive to grain size, particularly at lower temperatures. The fine-grained material can tolerate higher damage before fracture. Finally, the optimized hot-working process was determined.

DOI: 10.1007/s11661-014-2290-5

I. INTRODUCTION

HIGH-NITROGEN CrMn austenitic stainless steel (HNAS) has an interesting combination of mechanical, chemical, and physical properties: high strength and toughness, good corrosion resistance, and low magnetic susceptibility.[1] It has been widely used in the energy industries. However, surface cracks and coarse-grained and mixed-grain structures occur easily during the hot-working process of HNAS, leading to high production costs and low efficiency.[2,3]

Dynamic recrystallization (DRX) is a characteristic phenomenon of medium- and low-stacking-fault energy metallic materials during the hot-forming process and is of importance for two main reasons. The first is to soften and restore material ductility. The second is to control the grain structure by replacing initial coarse grains with small DRX grains.[4] Therefore, a study of factors affecting DRX in HNAS can promote the use of it to a large extent. Wang *et al.*,[2] Lang *et al.*,[5] and Hong *et al.*[6] investigated the effect of deformation parameters on the DRX behaviors of HNASs. Grain size as well as deformation parameters also influences the DRX behaviors.[7–13] However, limited information exists in the published literatures related to the grain size effect on the DRX and hot ductility behaviors in HNAS.

In fact, the effect of grain size on DRX in metallic materials is still being debated. In terms of DRX mechanism, Manshadi and Hodgson[8] found an interesting transition from ordinary to continuous DRX with a decrease in the initial grain size. However, Jafari and Najafizadeh[14] summarized that fine-grained initial structure favors ordinary DRX. In terms of DRX grain size, for high-purity[7] and ordinary[8,9] 304 austenitic stainless steels, the DRX grains evolved in fine-grained specimens are much smaller than those in the coarse-grained specimens. However, there is no major difference in DRX grain size between the two initial grain sizes in ultrahigh-purity 304 austenitic stainless steel.[7] This phenomenon also exists in some ordinary 304 austenitic stainless steels[10,11] and in Mg alloy.[12] In contrast, the initial coarse-grained material results in a finer DRX grain size than material with a finer starting microstructure in pure Ni.[13]

In this study, the dependences of DRX and hot ductility on the grain size of a HNAS (18Mn18Cr0.5N steel) are investigated. The main aim is to provide information to assist in establishing the hot-working process of HNAS components and resolving the above debate.

ZHENHUA WANG, Associate Professor, is with the State Key Laboratory of Metastable Materials Science and Technology, Yanshan University, Qinhuangdao 066004, P.R. China, and also with the Key Laboratory of Advanced Forging & Stamping Technology and Science, Yanshan University, Ministry of Education of China. SHUHUA SUN and WANTANG FU, Professors, and BO WANG and RONGHUA ZHANG, Students, are with the State Key Laboratory of Metastable Materials Science and Technology, Yanshan University. Contact e-mail: wtfu@ysu.edu.cn; wzh.ysu@163.com ZHONGPING SHI, Student, is with the Key Laboratory of Advanced Forging & Stamping Technology and Science, Yanshan University, Ministry of Education of China.

Manuscript submitted January 4, 2014.
Article published online April 5, 2014

II. EXPERIMENTAL MATERIAL AND PROCEDURE

The investigated 18Mn18Cr0.5N steel was melted in a vacuum-induction furnace. After electroslag remelting, its chemical composition was (wt pct): 0.11 C, 18.46 Mn, 18.5 Cr, 0.54 N, 0.71 Si, 0.02 P, 0.01 S, 0.01 Al, and balance Fe. Slabs were cut from the ingot and rolled at 1273 K (1000 °C). The cumulative deformation was approximately 1.6.

The rolled slabs were held at 1373 K (1100 °C) for 10 minutes, resulting in a homogenized microstructure with average grain size of 37 μm. To obtain a larger grain size, the slabs were held at 1473 K (1200 °C) for 120 minutes, resulting in the formation of coarse grains (160 μm). Hot compression specimens ($\Phi 10 \times 15$ mm) were cut parallel to the rolling direction. Hot compression tests were conducted on a Gleeble-3500 thermal/mechanical simulator. Graphite foil was used as a lubricant between the specimen and compression dies. Specimens were preheated at a rate of 10 K s^{-1} (°C s^{-1}) to 1273 K to 1473 K (1000 °C to 1200 °C). Thereafter, compression tests were performed at 0.1 s^{-1}. The specimens were deformed to a strain of 0.2 to 0.8 and then quenched immediately in water.

The deformed specimens were sectioned parallel to the direction of compression. The microstructures were observed using optical microscopy and electron backscatter diffraction (EBSD) analysis. EBSD analyses were performed using TSL-OIM Analysis software (EDAX Inc., Mahwah, NJ) to investigate specimens with a spatial resolution of 0.5 to 2 μm and misorientation detection limit of 1 deg. The crystal orientation maps display high-angle grain boundaries (misorientations ≥ 15 deg, shown as black lines), twin boundaries (shown as white lines), and low-angle grain boundaries (2 deg ≤ misorientations < 15 deg, shown as red lines). Transmission electron microscopy (TEM), using a JEM-2010 instrument (JEOL Ltd., Tokyo, Japan), was used to examine the grain boundaries.

To investigate the grain size effect on the hot ductility of 18Mn18Cr0.5N steel, tensile specimens ($\Phi 6 \times 120$ mm) were preheated to 1273 K to 1473 K (1000 °C to 1200 °C) at a rate of 10 K s^{-1} (°C s^{-1}) and pulled to fracture at a strain rate of 0.1 s^{-1}. The fracture surfaces were examined by scanning electron microscopy using a Hitachi S4800 instrument (Hitachi, Tokyo, Japan). The hot ductility was quantified in terms of the reduction in area at fracture. The deformed specimens were longitudinally sectioned. After being etched, the microstructures were observed near the fracture surface using optical microscopy.

III. RESULTS

A. *DRX Behaviors*

1. *Flow curves*

Figure 1 shows the flow curves of 18Mn18Cr0.5N steel with different initial grain sizes deformed at 1273 K to 1473 K (1000 °C to 1200 °C).

It is worth noting that the hardening rate after yield corresponding to the coarse initial grain size is higher.

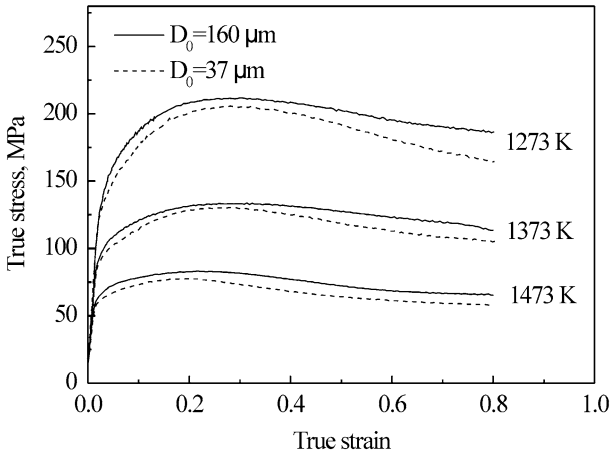

Fig. 1—Flow curves of 18Mn18Cr0.5N steel deformed at 1273 K to 1473 K (1000 °C to 1200 °C), D_0 denotes initial grain size.

This phenomenon is the same as that in References 8, 9, 12, and 13 but is contrary to References 7 and 10. In Reference 15, there is no regularity in the effect of the initial grain size on the hardening rate. The coarse initial grain size delayed the initiation of DRX, which is the same as reported in References 7 through 10, 12, and 13.

2. *DRX kinetics*

The DRX volume fraction follows the Avrami equation, $X = 1 - \exp[0.693(t/t_{0.5})^n]$, where X is the DRX volume fraction, $t_{0.5}$ is the time taken for 50 pct recrystallization, and n is the Avrami exponent. Assuming that the mechanical softening observed on the flow curves is directly related to the DRX volume fraction, the flowing constitutive equation provides the recrystallized fraction at any strain beyond the DRX initiation point[7,8,14]: $X = (\sigma_s - \sigma)/(\sigma_s - \sigma_{ss})$, where σ_{ss} is the steady-state stress at large strains and σ_s the saturation stress in the absence of DRX, which for practical purposes is associated here with the peak stress σ_p. The Avrami exponent was determined from the slope of the plot of $\log\{\ln[1/(1-X)]\}$ *vs* $\log[(\varepsilon - \varepsilon_p)/\dot{\varepsilon}]$, as shown in Figure 2. When no steady stress appears (no full DRX occurs), X under different strain conditions was determined by quantitative metallography.

The Avrami exponents obtained for both the fine- and coarse-grained materials were plotted as a function of deformation temperature in Figure 3. At 1273 K (1000 °C), n for the fine- and coarse-grained materials are 1.5 and 0.9, respectively. At 1373 K (1100 °C), their deference is pronounced. At 1473 K (1200 °C), they are close. The effect of initial grain size is considerable with the fine-grained materials having a higher n value, indicating a higher rate of DRX than in the coarse-grained material.

3. *Microstructure evolutions*

Figure 4 shows the microstructure of 18Mn18Cr0.5N steel deformed at 1273 K to 1473 K (1000 °C to 1200 °C) to a strain of 0.8, with two initial grain sizes of 37 and 160 μm. At 1273 K (1000 °C), the deformed microstructure corresponding to a coarse initial grain size (Figure 4(a)) consists of elongated parent grains surrounded by fine DRX grains, *i.e.,* necklace DRX.[2,14] More small grains form in the

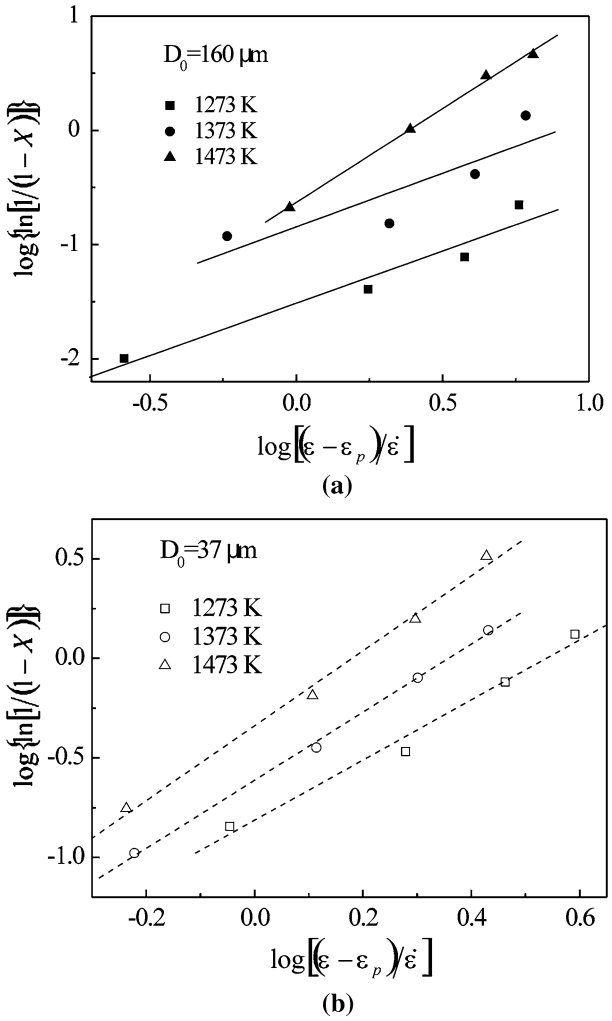

Fig. 2—Relationships between $\log\{\ln[1/(1-X)]\}$ and $\log[(\varepsilon-\varepsilon_p)/\dot{\varepsilon}]$ for 18Mn18Cr0.5N steel with different initial grain sizes: (*a*) 160 μm and (*b*) 37 μm.

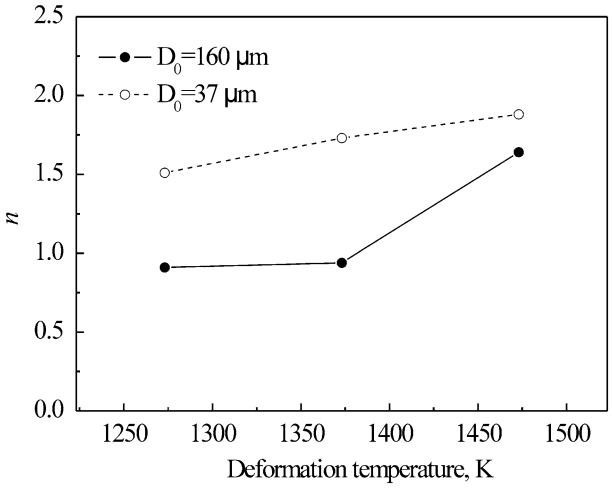

Fig. 3—Dependence of Avrami exponent on temperature for 18Mn18Cr0.5N steel with different initial grain sizes.

fine-grained specimen (Figure 4(b)). The DRX grain size and volume fraction increase with increasing deformation temperature (Figures 4(c) and (d)). Complete DRX has taken place in both fine- and coarse-grained specimens at 1473 K (1200 °C) (Figures 4(e) and (f)).

DRX grain sizes were obtained by the linear intercept method, as a function of temperature for 18Mn18Cr0.5N steel with different initial grain sizes after deformation to a strain of 0.8 (Figure 5). At 1273 K and 1473 K (1000 °C and 1200 °C), no effect of initial grain size was observed. In contrast, at 1373 K (1100 °C), larger DRX grains were observed for the coarse initial grain size condition.

4. *DRX mechanism*

Because the initial grain size has a pronounced effect on the DRX grain size at 1373 K (1100 °C), the microstructure evolutions of specimens with different initial grain sizes were investigated using EBSD analysis. In Figure 6(a) [1373 K (1100 °C)], the deformed microstructure corresponding to a coarse initial grain size (strain of 0.8) consists of elongated initial grains surrounded by fine DRX grains, *i.e.,* necklace DRX. Many low-angle grain boundaries exist in the deformed initial grains and no twin boundaries are observed. The nucleation of necklace DRX grains is mainly accompanied by the evolution of low-angle grain boundaries (separation mechanism[16,17]). Under initial fine-grain size condition (Figure 6(b)), DRX grains are formed at triple junctions (strain of 0.25), *i.e,.* ordinary DRX.[2,14] It is worth noting that the nucleation of DRX grains at triple junctions is mainly accompanied by the evolution of twinning (indicated by arrows). In the deformed initial grains, almost no low-angle boundaries are observed.

The specimen with fine initial grain size was compressed at 1273 K (1000 °C) to a strain of 0.4, to identify whether the nucleation mechanism of the DRX grains only depends on the initial grain size. In this case, necklace DRX occurs in the initial fine-grained material (Figure 6(c)). The nucleation of DRX grains is mainly accompanied by the evolution of low-angle grain boundaries. For 18Mn18Cr0.5N steel, the nucleation of DRX grains at triple junctions and at grain boundaries was mainly accompanied by the evolution of twinning and low-angle grain boundaries, respectively.

B. *Hot Ductility Behaviors*

1. *Reduction in area*

Figure 7 shows the hot ductility of 18Mn18Cr0.5N steel with two initial grain sizes, as a function of temperature. For the fine initial grain size condition, the material has an excellent ductility (> 90 pct) over the entire range of test temperatures. By comparison, the hot ductility is significantly lower in coarse-grained material. The reduction in area decreases with decreasing temperature. Obviously, the hot ductility of 18Mn18Cr0.5N steel is very sensitive to grain size, particularly at lower temperature.

2. *Fracture morphology*

Figure 8 shows the fracture surface of 18Mn18Cr0.5N steel with two initial grain sizes tensioned at 1273 K

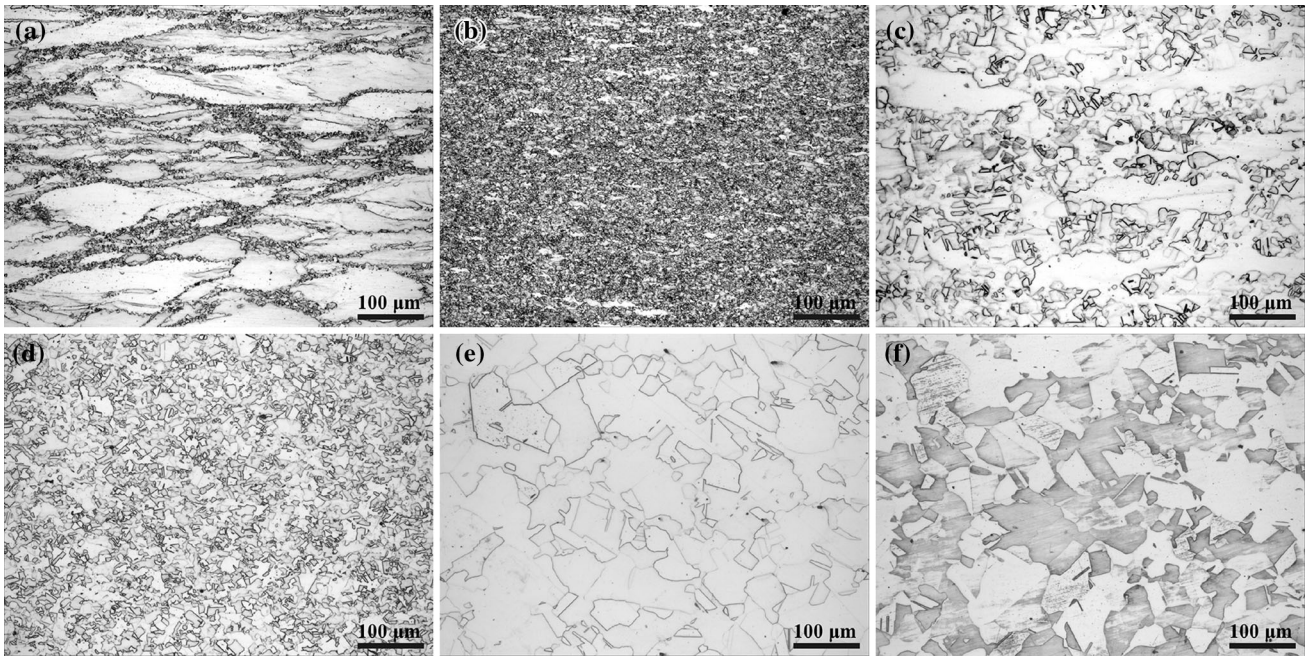

Fig. 4—Microstructure of 18Mn18Cr0.5N steel deformed to a strain of 0.8 with two initial grain sizes: (*a*) 1273 K (1000 °C), 160 μm; (*b*) 1273 K (1000 °C), 37 μm; (*c*) 1373 K (1100 °C), 160 μm; (*d*) 1373 K (1100 °C), 37 μm; (*e*) 1473 K (1200 °C), 160 μm; and (*f*) 1473 K (1200 °C), 37 μm.

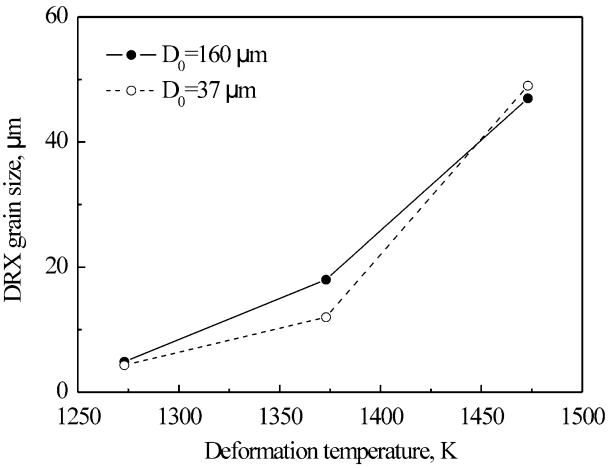

Fig. 5—Dependence of DRX grain size on initial grain size and deformation temperature (strain of 0.8), D_0 denotes initial grain size.

(1000 °C). Figure 8(a) (coarse grained) shows that the fracture exhibited features indicative of a combination of brittle and ductile mechanisms. The former is confirmed by the flat facet and the latter by the small dimples. A high-magnification image of this fracture surface is shown in Figure 8(b). In nature, the facet is the grain surface and the large edge is the grain edge. Figure 8(c) (fine grained) shows that the fracture surface is covered with many dimples and a high density of tearing edges, which are typical characteristics of ductile fracture.[18] A high-magnification image of this fracture surface is shown in Figure 8(d). Several small dimples are distributed at the bottom of large dimple. The occurrence of plane sliding is noted on the inner walls of the dimples.

Figure 9 shows the fracture surface of 18Mn18Cr0.5N steel with two initial grain sizes tensioned at 1373 K (1100 °C). In Figure 9(a) (coarse grained), the fracture surface exhibits a higher ductility than that in Figure 8(a). No flat facet can be observed. High-magnification imaging

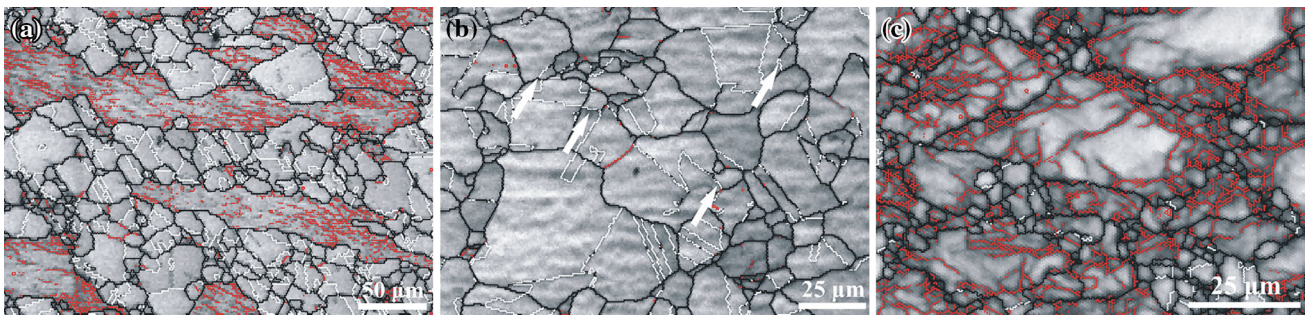

Fig. 6—EBSD maps of 18Mn18Cr0.5N steel deformed to different strains, with two initial grain sizes: (*a*) 1373 K (1100 °C), 160 μm, strain of 0.8; (*b*) 1373 K (1100 °C), 37 μm, strain of 0.25; and (*c*) 1273 K (1000 °C), 37 μm, strain of 0.4.

revealed the wavy and rough surface (Figure 9(b)). In Figure 9(c) (fine grained), the fracture surface exhibits many dimples. At a high magnification (Figure 9(d)), the fracture surface shows similar characteristics with that at 1273 K (1000 °C) (Figure 8(d)).

Figure 10 shows the fracture surface of 18Mn18Cr0.5N steel with two initial grain sizes tensioned at 1473 K (1200 °C). In Figure 10(a) (coarse grained), no dimple was observed on the rough fracture surface. At high magnification (Figure 10(b)), the fracture surface comprised refined grains with secondary cracks and voids around them. At 1473 K (1200 °C), fine- and coarse-grained materials show similar ductility (Figure 7), and their fracture morphologies are similar both at lower and higher magnifications (Figures 10(c) and (d)).

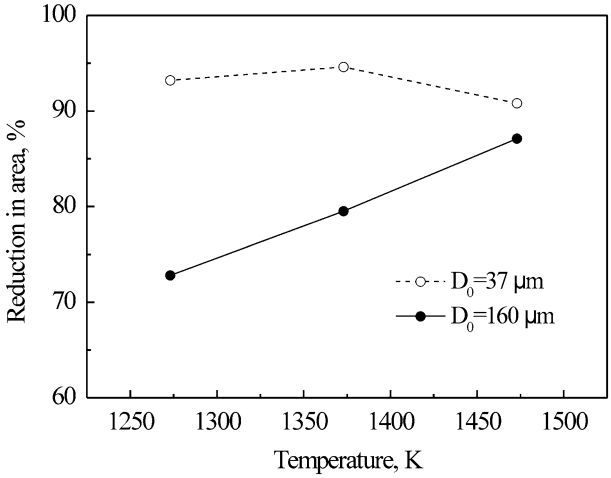

Fig. 7—Hot ductility curves of 18Mn18Cr0.5N steel with different initial grain sizes.

3. *Microstructure features of cracks*

Figure 11 shows the morphology in the vicinity of the fracture of specimens with two initial grain sizes. At 1273 K (1000 °C), the large parent grains are elongated and a small amount of grains formed through DRX are observed in coarse-grained material (Figure 11(a)). Large and long voids are distributed along grain boundaries. Intergranular cracks form through the accumulation of dislocations and voids at the grain boundary. In contrast, small voids are randomly distributed in the fine-grained materials (Figure 11(b)).

At 1373 K (1100 °C), the DRX extent and void density are both higher in coarse-grained material (Figure 11(c)) compared to those in Figure 11(a) [1273 K (1000 °C)]. This can explain why the reduction in area increases with increasing temperature in coarse-grained material. A large number of big voids exists in the vicinity of the fracture of specimens with fine-grained structure (Figure 11(d)). The elongated voids indicate that the fine-grained material undergoes a large amount of deformation after the initiation of cracking. At 1473 K (1200 °C), full DRX occurs in both fine- and coarse-grained specimens (Figures 11(e) and (f)). In this case, their microstructure features are similar in the vicinity of the fracture.

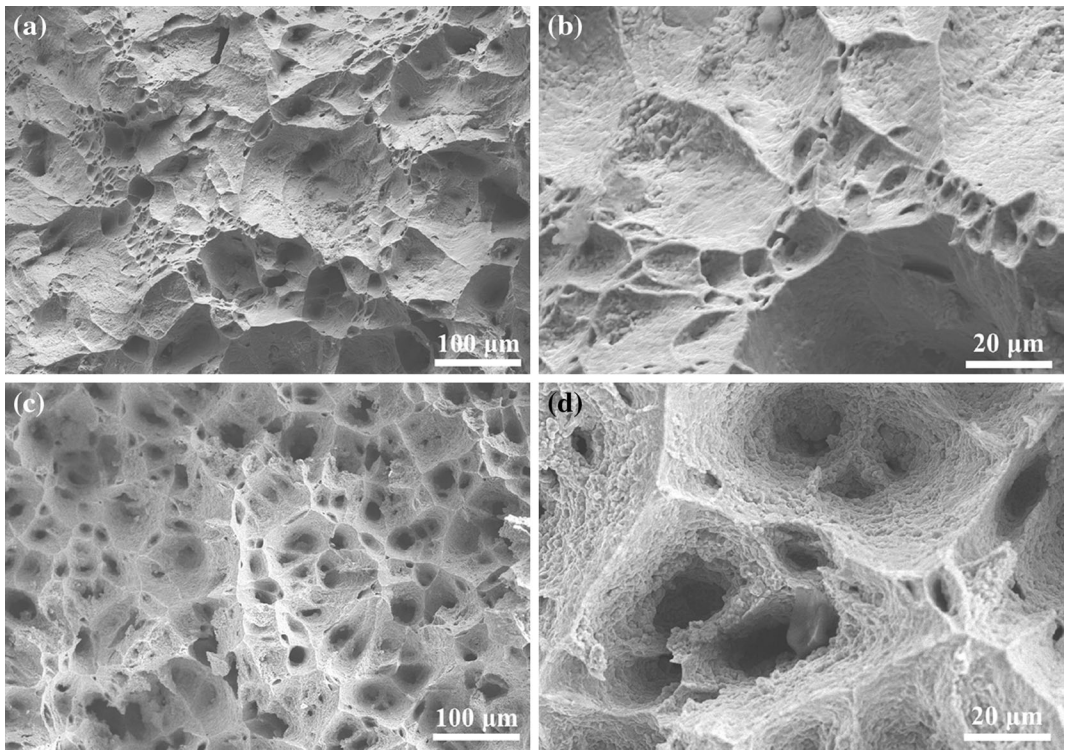

Fig. 8—Fracture surfaces of specimens tested at 1273 K (1000 °C): (*a*) and (*b*)160 μm, (*c*) and (*d*) 37 μm.

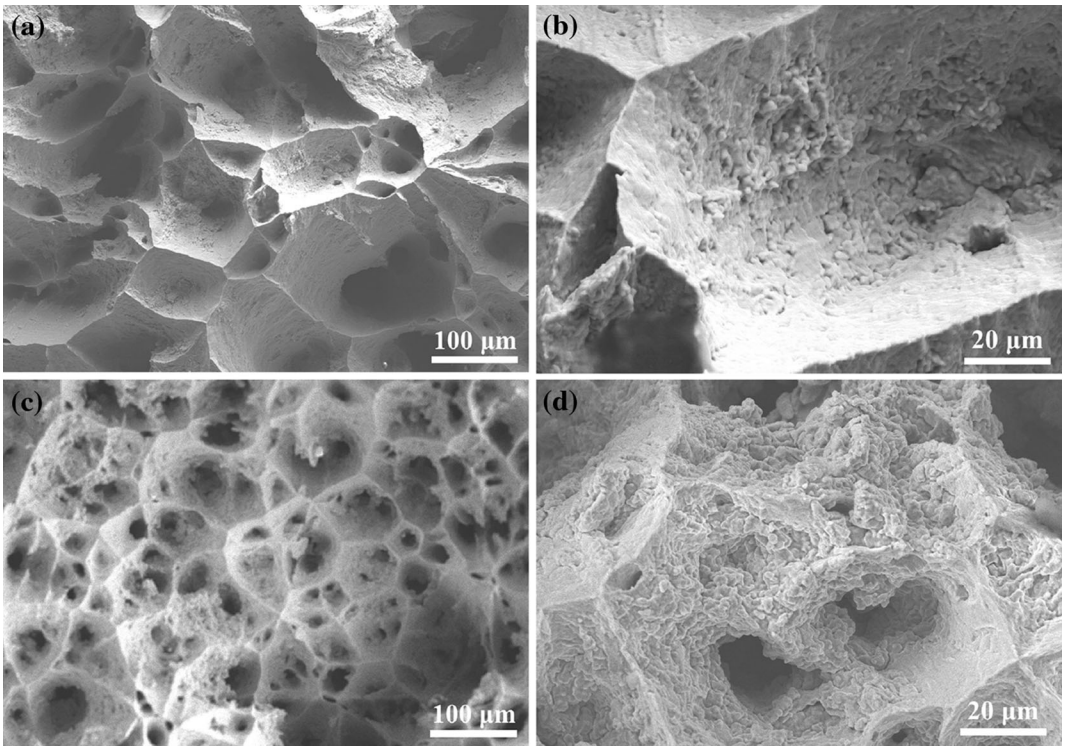

Fig. 9—Fracture surfaces of specimens tested at 1373 K (1100 °C): (*a*) and (*b*)160 μm, (*c*) and (*d*) 37 μm.

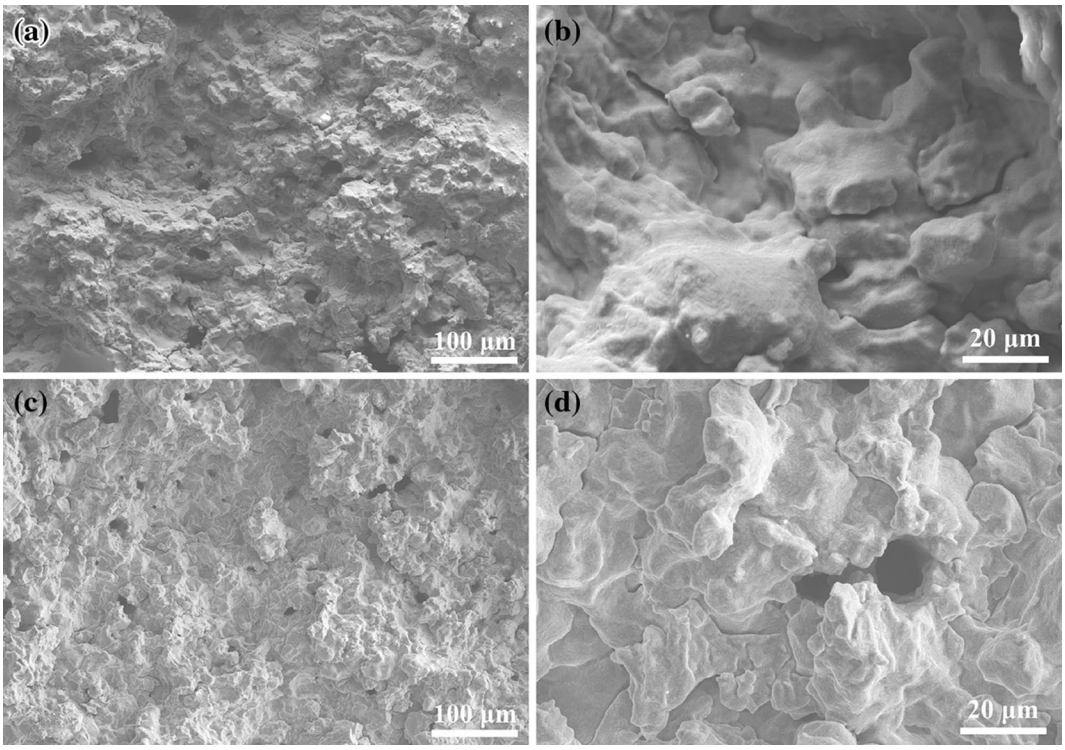

Fig. 10—Fracture surfaces of specimens tested at 1473 K (1200 °C): (*a*) and (*b*)160 μm, (*c*) and (*d*) 37 μm.

IV. DISCUSSION

A. *Effect of Grain Size on DRX Mechanism*

Based on the literature[7,14] and the above results, the grain size effect on DRX mechanism is schematically shown in Figure 12. The nucleation mechanism of DRX grains is affected not only by initial grain size but also by deformation condition (Zener-Hollomon parameter Z). It is worth noting that a transition region[19] may exist between two different regions.

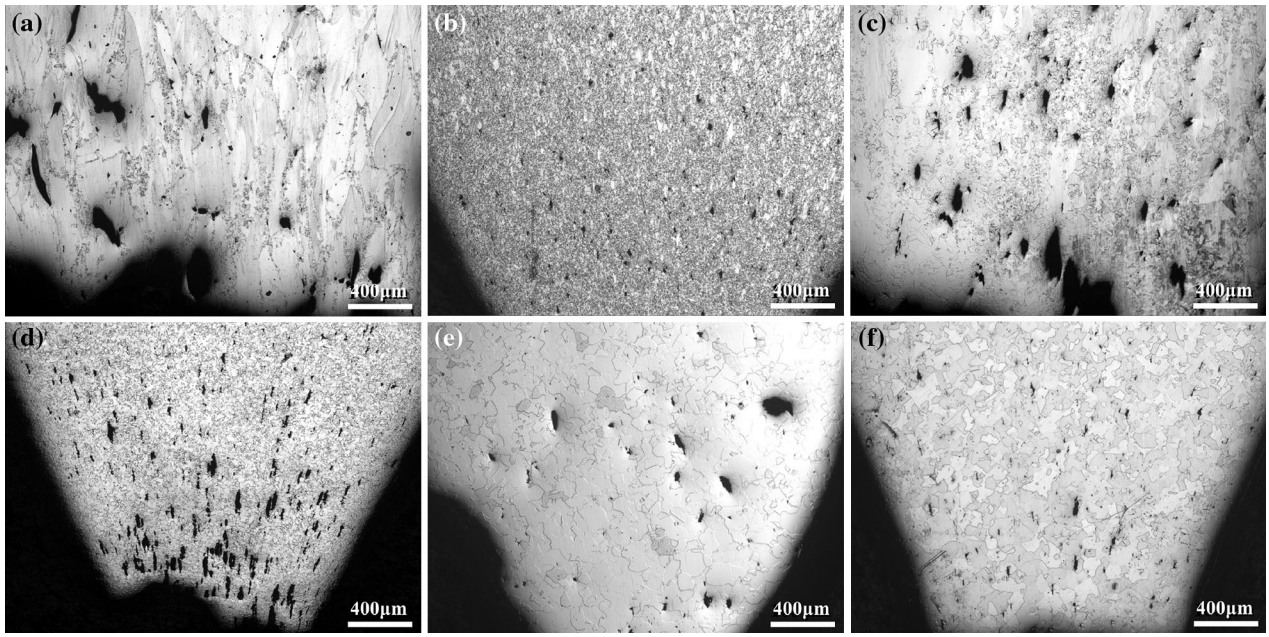

Fig. 11—Longitudinal cross sections of specimen fractures at (*a*) 1273 K (1000 °C), 160 μm; (*b*) 1273 K (1000 °C), 37 μm; (*c*) 1373 K (1100 °C), 160 μm; (*d*) 1373 K (1100 °C), 37 μm; (*e*) 1473 K (1200 °C), 160 μm; and (*f*) 1473 K (1200 °C), 37 μm.

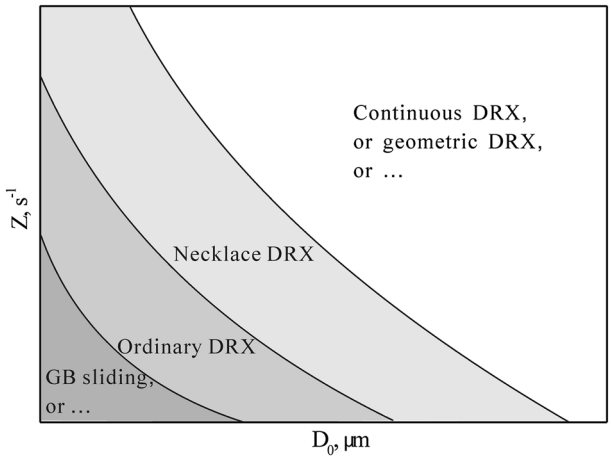

Fig. 12—Schematic drawing showing the effect of initial grain size and deformation conditions on the nucleation mechanism of DRX grains, GB denotes grain boundary.

B. *Effect of DRX Mechanism on DRX Grain Size*

At 1273 K (1000 °C), necklace DRX occurs simultaneously in materials with two initial grain sizes, and the DRX grain sizes are similar. At 1373 K (1100 °C), different DRX types induce different DRX sizes. At 1473 K (1200 °C), similar DRX grain sizes may result from the same DRX type (ordinary type).[2] It seems that different nucleation mechanisms induce various DRX grain sizes.

Figure 13 shows the TEM micrograph of a specimen deformed at 1273 K (1000 °C) to a strain of 0.4, with initial fine grain size. The curvature of the bulging portion is higher at the triple junction than at the grain boundary. In a fully recrystallized structure, the system energy is concentrated mainly at the grain boundaries. Triple junctions have a higher energy than that at grain boundaries. During deformation, the curvature of the bulging portion at the triple junctions is higher because of its higher energy and strain concentration. Smaller nuclei and more nucleation sites induce finer DRX grains,[7,8] which may explain why the DRX grains evolved by the ordinary mechanism are finer than those evolved by the necklace mechanism. From Figure 6(a), it can be seen that several newly formed DRX grains (next to parent grains) are in size of about 50 μm and much larger than those in the necklace region.

At a given Z, if the nucleation mechanisms of DRX grains in materials with two initial grain sizes are the same, then the DRX grain sizes are similar. When the nucleation mechanisms differ, the DRX grain size varies. This inference can explain why the effect of initial grain size on DRX grain size is so complex.[7–13]

In this study, if the strain is sufficiently large at 1373 K (1100 °C), then the influence of initial grain size on DRX grain size will be small. When the coarse parent grains are consumed, newly formed grains are still deformed and DRX will occur mainly at the triple junctions and be of the ordinary type. The final DRX grain size and final system energy will be similar to that of the initial fine-grained material. Therefore, the initial fine-grained material (higher initial system energy) shows a lower average deformation resistance (Figure 1).

C. *Effect of Grain Size on Hot Ductility*

Hot ductility is improved by DRX, which consumes damage and alleviates stress concentration at grain boundaries.[4] Increasing grain size increases the extent of inhomogeneous deformation and delays the initiation

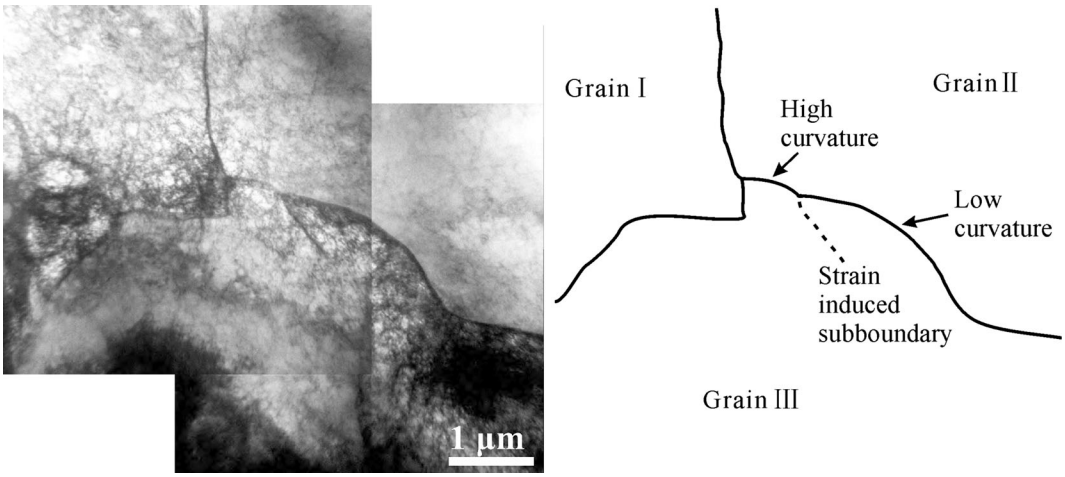

Fig. 13—TEM map of 18Mn18Cr0.5N steel deformed at 1273 K (1000 °C) to a strain of 0.4, with initial grain size of 37 μm.

and development of DRX. Therefore, fine-grained material exhibits better hot ductility. In addition, it can be found that fine-grained material tolerates higher damage before fracture. This is confirmed by the larger volume fraction of voids in the vicinity of the fracture, especially at 1373 K (1100 °C).

The cohesive strength of the grain boundaries may be weakened at 1473 K (1200 °C). Although DRX occurs easily, high triaxial stress will lead to sudden fracture when the necking reaches a certain level. In Figures 11(e) and (f), only a few small voids are observed in the vicinity of the fracture. This observation is consistent with Faccoli and Roberti's work,[20] where it was found that the void density is highly sensitive to strain at higher temperatures; that is, the number of cracks decreases quickly from the fracture surface to the specimen interior.

D. *Optimized Hot-Working Process*

In the hot-working process of 18Mn18Cr0.5N steel component, especially heavy forging, the grain structure of component surface should be refined in the early stages of deformation [in the high-temperature range, ca. 1473 K (1200 °C)]. This is because the hot ductility of 18Mn18Cr0.5N steel component with a coarse grain structure dramatically decreases with decreasing temperature. If the surface coarse grains were refined, then the surface cracking will be restrained in the lower temperature range.

V. CONCLUSIONS

1. For 18Mn18Cr0.5N steel, the coarse initial grain size delays the initiation and development of DRX.
2. The nucleation of DRX grains at triple junctions and at grain boundaries is mainly accompanied by the evolution of twinning and low-angle grain boundaries, respectively.
3. The nucleation mechanism of DRX grains affects the DRX grain size. DRX evolved by the necklace mechanism are coarser than those evolved by the ordinary mechanism.
4. The fine-grained material tolerates higher damage before fracture and results in a higher hot ductility.
5. The hot ductility of HNAS is very sensitive to grain size, particularly at lower temperature. The grain structure of HNAS component surface should be refined in the early stages of deformation.

ACKNOWLEDGMENTS

The project is supported by the Natural Science Foundation of Hebei Province for Distinguished Young Scholars (E2011203131) and the Natural Science Foundation–Steel and Iron Foundation of Hebei Province (E2013203110).

REFERENCE

1. J.W. Simmons: *Mater. Sci. Eng. A*, 1996, vol. 207, pp. 159–69.
2. Z.H. Wang, W.T. Fu, S.H. Sun, H. Li, Z.Q. Lv, and D.L. Zhao: *Metall. Mater. Trans. A*, 2010, vol. 41A, pp. 1025–32.
3. Z.H. Wang, W.T. Fu, S.H. Sun, Z.Q. Lv, and W.H. Zhang: *J. Mater. Sci. Technol.*, 2010, vol. 26, pp. 798–802.
4. R.D. Doherty, D.A. Hughes, F.J. Humphreys, J.J. Jonas, D. Juul Jensen, M.E. Kassner, W.E. King, T.R. McNelley, H.J. McQueen, and A.D. Rollett: *Mater. Sci. Eng. A*, 1997, vol. 238, pp. 219–74.
5. Y.P. Lang, Y. Zhou, F. Rong, H.T. Chen, Y.Q. Weng, and J. Su: *J. Iron Steel Res. Int.*, 2010, vol. 17, pp. 45–49.
6. C.M. Hong, J. Shi, L.Y. Sheng, W.C. Cao, W.J. Hui, and H. Dong: *Mater. Des.*, 2011, vol. 32, pp. 3711–17.
7. M. El Wahabi, L. Gavard, F. Montheillet, J.M. Cabrera, and J.M. Prado: *Acta Mater.*, 2005, vol. 53, pp. 4605–12.
8. A.D. Manshadi and P.D. Hodgson: *Metall. Mater. Trans. A*, 2008, vol. 39, pp. 2830–40.
9. A. Belyakov, H. Miura, and T. Sakai: *Scripta Mater.*, 2000, vol. 43, pp. 21–26.
10. A. Belyakov, K. Tsuzaki, H. Miura, and T. Sakai: *Acta Mater.*, 2003, vol. 51, pp. 847–61.
11. A.D. Manshadi, M.R. Barnett, and P.D. Hodgson: *Mater. Sci. Eng. A*, 2008, vol. 485, pp. 664–72.
12. M.R. Barnett, A.G. Beer, D. Atwell, and A. Oudin: *Scripta Mater.*, 2004, vol. 51, pp. 19–24.

13. C. Rehrl, S. Kleber, O. Renk, and R. Pippan: *Mater. Sci. Eng. A*, 2011, vol. 528, pp. 6163–72.
14. M. Jafari and A. Najafizadeh: *Mater. Sci. Eng. A*, 2009, vol. 501, pp. 16–25.
15. C. Rehrl, S. Kleber, O. Renk, and R. Pippan: *Mater. Sci. Eng. A*, 2012, vol. 540, pp. 55–62.
16. A.M.W. Sarnek, H. Miura, and T. Sakai: *Mater. Sci. Eng. A*, 2002, vol. 323, pp. 177–86.
17. A. Belyakov, H. Miura, and T. Sakai: *Mater. Sci. Eng. A*, 1998, vol. 255, pp. 139–47.
18. J. Deng, Y.C. Lin, S.S. Li, J. Chen, and Y. Ding: *Mater. Des.*, 2013, vol. 49, pp. 209–19.
19. N. Dudova, A. Belyakov, T. Sakai, and R. Kaibyshev: *Acta Mater.*, 2010, vol. 58, pp. 3624–32.
20. M. Faccoli and R. Roberti: *J. Mater. Sci.*, 2013, vol. 48, pp. 5196–203.